



Permian plume beneath Tarim from receiver functions

Lev Vinnik¹, Yangfan Deng², Grigoriy Kosarev¹, Sergey Oreshin¹, Larissa Makeyeva¹

1. Institute of physics of the Earth, Russian Academy of Sciences, Moscow, Russia
2. State Key Laboratory of Isotope Geochemistry, Guangzhou Institute of Geochemistry,
5 Chinese Academy of Sciences, Guangzhou 510640, China

Correspondence to: Yangfan Deng (Yangfandeng@gig.ac.cn) and Lev Vinnik (vinnik@ifz.ru)

Abstract

Receiver functions for the central Tien Shan and northern Tarim in central Asia reveal a pronounced depression on the 410-km discontinuity beneath the Permian basalts in Tarim. The 10 depression may most likely be caused by elevated temperature. The striking spatial coherence between the anomaly of the MTZ and the Permian basalts suggests that both may be effects of the same plume. This relation can be reconciled with reconstructed positions of paleo-continents since the Permian by assuming that the mantle layer which translated coherently with the Tarim plate extended to a depth of 410 km or more. Alternatively, lithosphere and the underlying 15 mantle are decoupled at a depth of ~ 200 km, but a cumulative effect of the Tarim plate motions since the Permian is by an order of magnitude less than predicted by the paleo-reconstructions. A similar explanation is applicable to the Siberian traps.

1. Introduction.

Theoretical considerations predict decoupling of the rigid lithosphere and the underlying ductile 20 upper mantle (asthenosphere) at the lithosphere-asthenosphere boundary (Eaton et al., 2009). The depth to the lithosphere-asthenosphere boundary (LAB) ranges from a few tens kilometers for a young lithosphere to about 300 km for Precambrian cratons (e.g. Artemieva and Mooney, 2001). Another idea postulates that the layer which translates coherently with the continental



plate (tectosphere) may extend to a depth of at least 400 km (Jordan, 1978). Examples of
25 successful application of the concept of tectosphere to geophysical data are few. We test this idea
by comparing the locations of possible remnants of extinct mantle plumes in the mantle
transition zone (MTZ) and the related basaltic outcrops at the Earth's surface.

Recently this test was applied to the Siberian Large Igneous Province (LIP). The Siberian
traps present the result of gigantic basalt eruptions which took place near the Permo-Triassic
30 boundary at about 250 Ma (Fedorenko et al., 1996). The analysis of structure of the mantle
beneath the Siberian LIP was conducted with the aid of receiver function techniques that were
applied to the recordings of seismograph station Norilsk (NRIL) within the Siberian LIP (Vinnik
et al., 2017). This analysis has shown that the seismic boundary at the top of the MTZ with a
standard depth of 410 km is depressed in the vicinity of NRIL by 10 km. The diagram of olivine
35 - wadsleyite phase transition may account for this depression by assuming about 100 K increase
of the temperature. In the depth range from 350 to 410 km, the S velocity in the region beneath
the Siberian LIP drops by a few percent. This effect is a likely result of partial melting (Hier-
Majumder and Courtier, 2011) which is unusual for cratons. Another low-velocity layer is found in
the depth interval from 460 to 500 km and may also be the result of partial melting. Similar
40 anomalies were previously found in the vicinities of several presently active hot-spots (Vinnik
and Farra, 2006). The Siberian Craton shifted in the last 250 Myr by about 2000 km to the east
(Torsvik et al., 2008). The anomalies of the MTZ might preserve their position beneath the
Siberian LIP in spite of the plate motion if they translated coherently with the Siberian plate.

A similar conclusion is obtained for Greenland by Kraft et al. (2018). Arrival times of
45 P660s and P410s mode converted phases in P receiver functions (PRFs) were measured at 24
seismograph stations in central-eastern Greenland. In two regions corresponding to basaltic
outcrops about 55 Myr old, the differential time between P660s and P410s seismic phases is
reduced by more than 2 s relative to IASP91 reference model. The 410-km discontinuity in these
regions is depressed by more than 20 km. The depression can be explained by elevated



50 temperature. The basaltic outcrops and the related temperature anomalies are likely related to the passage of Greenland over the Iceland hot-spot. This explanation is consistent with the concept of tectosphere and implies that the upper mantle beneath Greenland to a depth of at least 430 km translated coherently with the Greenland plate.

Here we use P receiver functions (PRFs) to do the similar analysis for the central Tien
55 Shan and Tarim in central Asia. And then we discuss the possible implications for the origin of the seismic features.

2. Seismic structure of the MTZ beneath the central Tien Shan and Tarim.

This section presents in condensed form the results of the recent seismic study (Kosarev et
50 al., 2018) of the MTZ beneath the central Tien Shan and northern Tarim (Fig.1). The ongoing orogenesis in central Asia is a likely far-field effect of the India-Eurasia collision (Molnar and Tapponnier, 1975). Previous mountain-building episodes in the region of the Tien Shan took place in the Paleozoic (e.g., Windley et al., 1990), but for about 100 Myr prior to the onset of the present-day mountain building the lithosphere of the Tien-Shan was quiet. Tectonic activity
55 resumed at about 25-20 Ma in the southern Tien Shan (Sobel and Dumitru, 1997) and at 11 Ma in the north (Bullen et al., 2001). The lithosphere of Tarim underthrusts the relatively weak lithosphere of the Tien Shan at a rate of about 20 mm/yr (Reigber et al., 2001).

Telesismic recordings of about 100 broad-band stations in Fig. 1 were low-pass filtered
70 with a corner at around 6 s and transformed into PRF. The PRFs were calculated by using the LQ coordinate system, where L is parallel to the principal motion direction of the P wave and Q is normal to L in the wave propagation plane. The Q components were deconvolved by the L components and stacked to reduce noise. In the context of our study the most important elements of the PRFs are P660s and P410s converted seismic phases. The 410-km and 660-km discontinuities mark the top and bottom of the MTZ and their depths are sensitive to the
75 temperature.



The times of P660s and P410s seismic phases depend not only on topography of the 660-km and 410-km discontinuities but also on volumetric velocity heterogeneities above the 410-km boundary. Separation of these two different effects is the main problem of interpreting the observations of these phases. The ray paths of the P660s and P410s phases in the same seismic recording are very close to each other at depths less than 410 km and, therefore, the time difference between them (differential time) depends mainly on the width of the MTZ. The study area was divided into rectangular boxes 2° in the SN and EW directions (220 and 160 km, respectively). The theoretical conversion points in the middle of the MTZ (535 km) for the standard reference model IASP91 were projected on the Earth's surface for all available recordings. Those PRFs, the projections of the conversion points of which fall in the same box, were stacked with move-out time corrections.

The number of the stacked PRFs in most of the boxes is on the order of several hundreds. These numbers are sufficient for a robust detection of P660s and P410s seismic phases (see example in Fig. 2). The accuracy of the estimates of the differential time (confidence interval of 90 66%) is typically 0.2 s. For most boxes the residuals of the differential time with respect to the IASP91 value (23.9 s) are on the order of a fraction of a second (Fig. 3). Large residuals (more than 1.0 s) are obtained for three boxes: (40° - 42°N, 76° - 78°E, +1.5 s), (40° - 42°N, 72° - 74°E, -1.1 s) and (38° - 40°N, 80° - 82°E, -1.5 s). The resulting anomalies of thickness of the MTZ are +15 km, -11 km, and -15 km, respectively. These anomalies are located beneath the south-central Tien Shan, Fergana Basin and Tarim, respectively.

The further analysis (Kosarev et al., 2018) demonstrates that the increased thickness of the MTZ beneath the south-central Tien Shan is the effect of an uplift of the 410-km discontinuity and a depression of the 660-km discontinuity. The MTZ might be cooled by a detached and sinking mantle lithosphere. The thinned MTZ beneath the Fergana and Tarim basins is the effect of a depressed 410-km discontinuity and a stable 660-km discontinuity. The depressed 410-km discontinuity beneath Fergana and Tarim is likely a result of a temperature



anomaly of about +100 °C. The elevated temperature beneath Fergana may be related to a plume which is responsible for small-scale basaltic volcanism in the Tien Shan from 72 Ma to 60 Ma. Possible origin of the anomaly beneath Tarim is discussed in next Section.

105

3. Possible origin of the anomalous MTZ beneath Tarim.

Tarim can be characterized as an Archean craton (Yuan et al., 2004) with a complex evolutionary history (Zhang et al., 2013; Deng et al., 2017). In the Permian, basalts with the areal extent of about 200000 km² erupted in the west of the Tarim basin (Fig. 4). The thickness of basalt reaches 110 700 m. The age span of the magmatism extends from about 290 Ma to 260 Ma, with a peak between 270 Ma and 280 Ma. The magmatism is interpreted as plume-induced (Zhang et al., 2010; Xu et al., 2014). Evidence for the mantle plume beneath Tarim includes high heat flow and uplift during the Permian. No magmatic activity in Tarim is known in the Cretaceous and Cenozoic (Deng et al., 2017).

115 Fig. 4 demonstrates a striking spatial coherence of the depressed 410-km discontinuity and the magmatic province in Tarim, with implication of a causal relation between them. The depressed 410-km discontinuity and the stable 660-km discontinuity are typical for hotspots and plumes (e.g. Du et al., 2006), though there are some exceptions (e.g. Vinnik et al., 2012). The stable depth of the 660-km discontinuity is either the result of a zero temperature anomaly at the 120 base of the MTZ or an effect of two phase transitions at nearly the same depth but with opposite Clapeyron slopes (Hirose, 2002).

The assumed causal relation between the Permian basalts and the present-day anomaly implies that the anomaly at a depth of ~400 km may exist for ~300 m.y. To check this possibility we calculated the temperature for 1D conductive medium by using the well known expression 125 $T(r,t) = Q \exp(-r^2/4\alpha t)/2\sqrt{\pi\alpha t}$, where T is temperature, t is time, r is distance, α is diffusivity, Q is constant, and the initial temperature anomaly distribution is taken in the form of δ -function at r



= 0 and $t = 0$. The diffusivity α is taken equal to $32 \text{ km}^2/\text{m.y.}$ The results (Fig.5a) demonstrate that the temperature anomaly in the time interval of 300 m.y. (between 100 m.y. and 400 m.y.) is reduced twice. The maximum temperature anomaly in plumes is $\sim 300 \pm 100^\circ\text{C}$ (Campbell, 2005), 130 which means that the temperature anomaly after 300 m.y. may be around 150°C , close to the seismic estimate. A comparable result is obtained for 2D conductive medium (Fig. 5b). These calculations suggest that the thermal anomaly at a depth of 400 km may survive for a few hundred million years.

It is also possible that the anomaly at a depth of ~ 400 km is an effect of chemical 135 composition. The pressure of the phase transition in $(\text{Mg},\text{Fe})_2\text{SiO}_4$ depends on the Mg content relative to Fe (Fei and Bertka, 1999). Increasing the Mg content from 89% to 92% results in up to 10-km deepening of the 410-km discontinuity (Schmerr and Garnero, 2007). The increased content of Mg in the plume may be a result of partial melting.

Relative positions of the present-day thermal anomaly in the MTZ and the Permian basalt 140 eruptions depend on plate motions in the last ~ 300 Myr. Reconstructions of positions of old continents is difficult for the time exceeding the age of the oldest hot-spot trails (130 Ma). There are abundant paleomagnetic data for the earlier times, but they do not constrain paleo-longitudes. The uncertainty can be minimized by selecting Africa as a reference continent that was most 145 stable longitudinally (Torsvik et al. 2008). In this reference frame the Siberian traps shifted to the east by nearly 2000 km since they were erupted at 250 Ma (Torsvik et al., 2008). Tarim and the Siberian craton were parts of the same continental plate in the past 300 Myr, and 2000 km can be used as a rough estimate of the shift of Tarim. Additionally, Tarim moved to the northeast as a result of the collision of India with Eurasia (Molnar and Tapponnier, 1975).

The spatial coherence between the anomaly in the MTZ and basalt eruptions in Tarim (Fig. 150 4) in spite of the shift of the Tarim craton to the east and north-east by a few thousand kilometers is possible if the layer which translates coherently with the plate includes the top of the MTZ. Alternatively this is possible without the recourse to the deep tectosphere, if the available paleo-



reconstructions for Asia are too rough and the actual shift of Tarim is by an order of magnitude less than predicted. This would also be true for the Siberian traps.

155 **4. Conclusions**

The striking spatial coincidence of the Permian basalts and a depression on the 410-km discontinuity beneath Tarim (Fig. 4) suggests that both may be related to the same mantle plume. This relation allows a dual interpretation. Recent reconstructions (Torsvik et al., 2008) demonstrate a shift of Tarim of about 2000 km in the past 300 Myr. Then the observed relation 160 between the deep and shallow features can be explained by a coherent translation of the crust and mantle to a depth of 430 km. Alternatively the spatial coincidence of the deep and shallow features is possible without the recourse to the deep tectosphere if the actual shift of Tarim is by an order of magnitude less than predicted by the reconstructions. Practically similar conclusions would apply to the Permo-Triassic traps of the Siberian Craton.

165 **Acknowledgment**

This study was supported by the joint project between Russian Foundation for Basic Research (RFBR, grant 17-55-53-117) and National Natural Science Foundation of China (NSFC, grant 41611530695), the Strategic Priority Research Program (B) of the Chinese Academy of Sciences (grant XDB18000000).

170

References

Artemieva, I. M., and Mooney, W. D.: Thermal thickness and evolution of Precambrian lithosphere: a global study, *Journal of Geophysical Research: Solid Earth*, 106(B8), 16387-16414, 2001

175 Bullen, M. E., Burbank, D. W., Garver, J. I., and Abdurakhmatov, K. Y.: Late Cenozoic tectonic evolution of the northwestern Tien Shan: New age estimates for the initiation of mountain building, *Geological Society of America Bulletin*, 113(12), 1544-1559, 2001.



Campbell, I. H.: Large igneous provinces and the mantle plume hypothesis, *Elements*, 1(5), 265-269, 2005.

180 Deng, Y., Levandowski, W., and Kusky, T.: Lithospheric density structure beneath the Tarim basin and surroundings, northwestern China, from the joint inversion of gravity and topography, *Earth and Planetary Science Letters*, 460, 244-254, 2017.

Du, Z., Vinnik, L. P., and Foulger, G. R.: Evidence from P-to-S mantle converted waves for a flat “660-km” discontinuity beneath Iceland, *Earth and Planetary Science Letters*, 241(1-2), 185 271-280, 2006.

Eaton, D. W., Darbyshire, F., Evans, R. L., Grüter, H., Jones, A. G., and Yuan, X.: The elusive lithosphere–asthenosphere boundary (LAB) beneath cratons, *Lithos*, 109(1-2), 1-22, 2009.

Fedorenko, V. A., Lightfoot, P. C., Naldrett, A. J., Czamanske, G. K., Hawkesworth, C. J., Wooden, J. L., and Ebel, D. S.: Petrogenesis of the flood-basalt sequence at Noril'sk, north 190 central Siberia, *International Geology Review*, 38(2), 99-135, 1996.

Fei, Y., and Bertka, C. M.: Phase transitions in the Earth's mantle and mantle mineralogy, *Mantle petrology: field observations and high pressure experimentation*, 6, 189-207, 1999.

Jordan, T. H.: Composition and development of the continental tectosphere, *Nature*, 274(5671), 544, 1978.

195 Hier-Majumder, S., and Courtier, A.: Seismic signature of small melt fraction atop the transition zone, *Earth and Planetary Science Letters*, 308(3-4), 334-342, 2011.

Hirose, K.: Phase transitions in pyrolytic mantle around 670 - km depth: Implications for upwelling of plumes from the lower mantle, *Journal of Geophysical Research: Solid Earth*, 107(B4), 2002.

200 Kosarev, G., Oreshin, S., Vinnik, L., and Makeyeva, L.: Mantle transition zone beneath the central Tien Shan: Lithospheric delamination and mantle plumes, *Tectonophysics*, 723, 172-177, 2018.



Kraft, H. A., Vinnik, L., and Thybo, H.: Mantle transition zone beneath central-eastern Greenland: Possible evidence for a deep tectosphere from receiver functions,
205 *Tectonophysics*, 728, 34-40, 2018.

Molnar P., and Tapponnier P.: Cenozoic tectonics of Asia: effects of a continental collision,
Science 189, 419-426, 1975.

Reigber, C., Michel, G., Galas, R., Angermann, D., Klotz, J., Chen, J., Papschev, A., Arslanov,
R., Tzurkov, V. and Ishanov, M.: New space geodetic constraints on the distribution of
210 deformation in Central Asia. *Earth and Planetary Science Letters*, 191(1-2), 157-165, 2001.

Schmerr, N., and Garnero, E. J.: Upper mantle discontinuity topography from thermal and
chemical heterogeneity, *Science*, 318(5850), 623-626, 2007.

Sobel, E. R., and Dumitru, T. A.: Thrusting and exhumation around the margins of the western
Tarim basin during the India-Asia collision, *Journal of Geophysical Research: Solid Earth*,
215 102(B3), 5043-5063, 1997.

Torsvik, T. H., Steinberger, B., Cocks, L. R. M., and Burke, K.: Longitude: linking Earth's
ancient surface to its deep interior, *Earth and Planetary Science Letters*, 276(3-4), 273-282,
2008.

Vinnik, L., and Farra, V.: S velocity reversal in the mantle transition zone, *Geophysical research
220 letters*, 33(18), 2006.

Vinnik, L., Silveira, G., Kiselev, S., Farra, V., Weber, M., and Stutzmann, E.: Cape Verde
hotspot from the upper crust to the top of the lower mantle, *Earth and Planetary Science
Letters*, 319, 259-268, 2012.

Vinnik, L. P., Oreshin, S. I., and Makeyeva, L. I.: Siberian traps: Hypotheses and seismology
225 data, *Izvestiya, Physics of the Solid Earth*, 53(3), 332-340, 2017.

Windley, B. F., Allen, M. B., Zhang, C., Zhao, Z. Y., and Wang, G. R.: Paleozoic accretion and
Cenozoic reformation of the Chinese Tien Shan range, central Asia. *Geology*, 18(2), 128-
131, 1990.



Xu, Y.-G., Wei, X., Luo, Z.-Y., Liu, H.-Q., and Cao, J.: The Early Permian Tarim Large Igneous
230 Province: main characteristics and a plume incubation model. *Lithos*, 204, 20–35, 2014.

Zhang, Y., Liu, J., & Guo, Z.: Permian basaltic rocks in the Tarim basin, NW China:
implications for plume–lithosphere interaction. *Gondwana Research*, 18(4), 596–610, 2010.

Yuan, C., Sun, M., Yang, J., Zhou, H., and Zhou, M.-F.: Nb-depleted, continental rift-related
Akaz metavolcanic rocks (West Kunlun): implication for the rifting of the Tarim Craton
235 from Gondwana. *Geological Society, London, Special Publications*, 226(1), 131–143, 2004.

Zhang, C.-L., Zou, H.-B., Li, H.-K., and Wang, H.-Y.: Tectonic framework and evolution of the
Tarim Block in NW China. *Gondwana Research*, 23(4), 1306–1315, 2013.

Figure captions

240 **Figure 1.** Topographic map of the study region and the seismograph network.

Figure 2. Stacked PRFs for the box with the coordinates: 38 N, 40N, 80 E and 82 E. Trial
conversion depths in kilometers for each trace are shown on the left-hand side. The detected
P410s and P660s phases are marked by arrows.

245 **Figure 3.** Residuals of the differential time between P660s and P410s phases in seconds relative
to IASP91. Strongly anomalous boxes are in south-central Tien Shan (1.5 s, blue), Fegana basin
(-1.1 s, red) and Tarim (-1.5 s, red). Light shading indicates elevations greater than 1500 m,
intermediate shading elevations greater than 3000 m.

Figure 4. Superimposed Permian basalts in Tarim (orange) and the anomalous region on the 410-
km discontinuity.

250 **Figure 5.** Temperature anomaly distributions in 1D (a) and 2D (b) conductive media with an
interval of 300 million years.



Figure 1

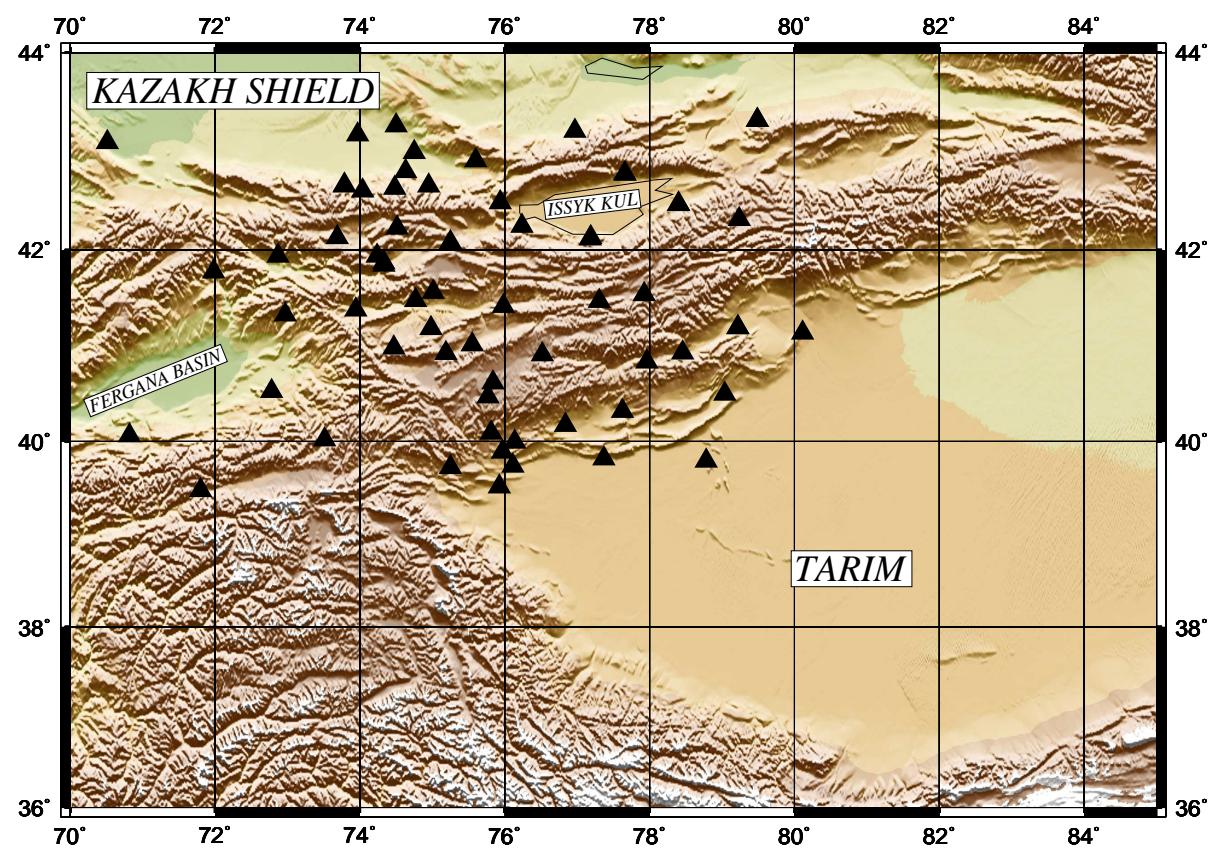




Figure 2

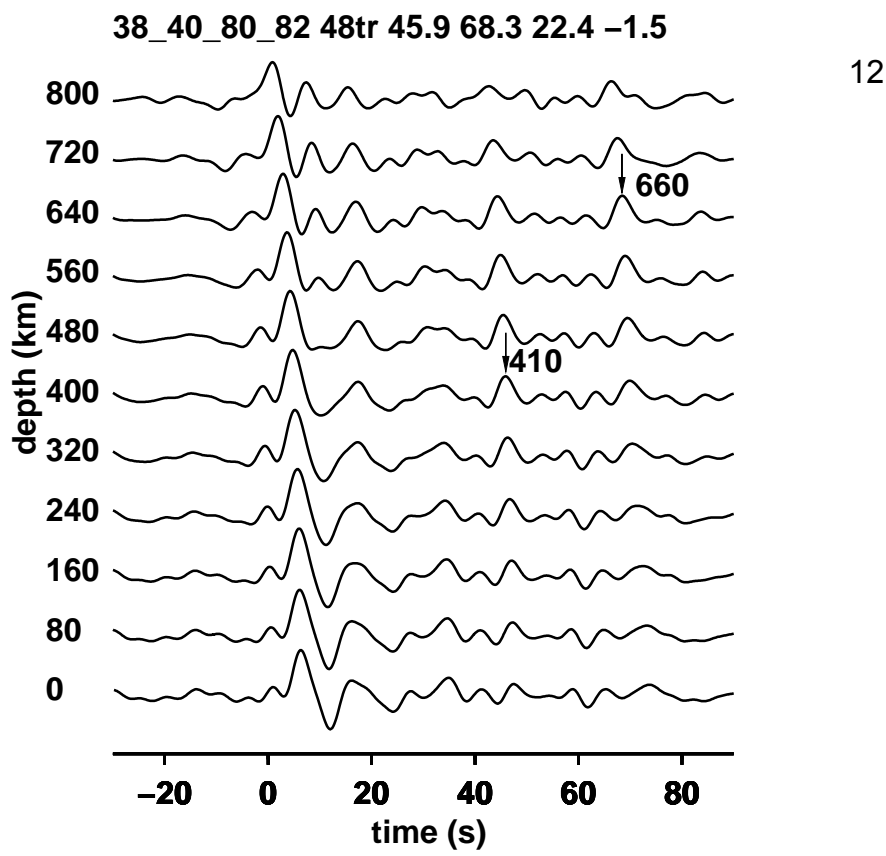




Figure 3

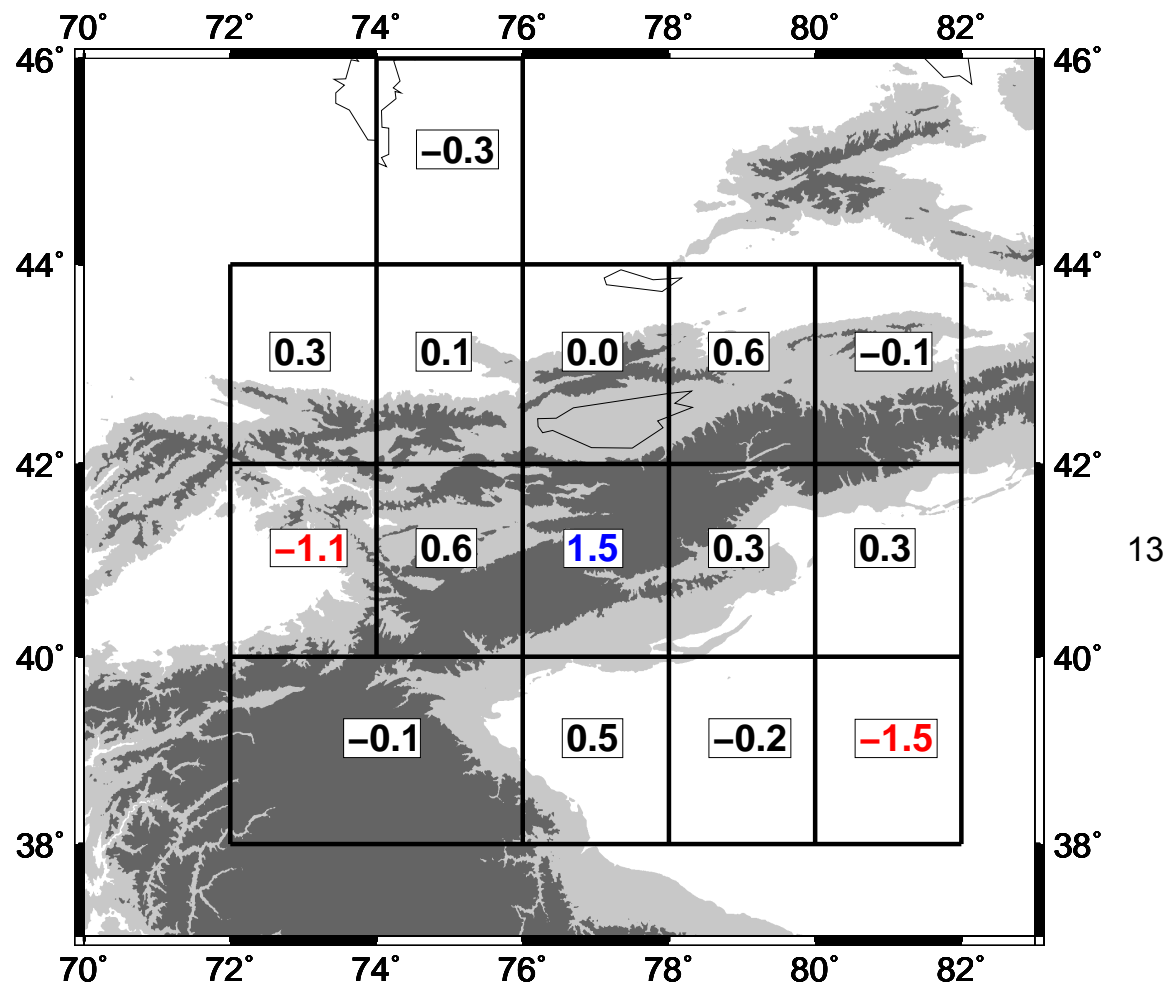




Figure 4

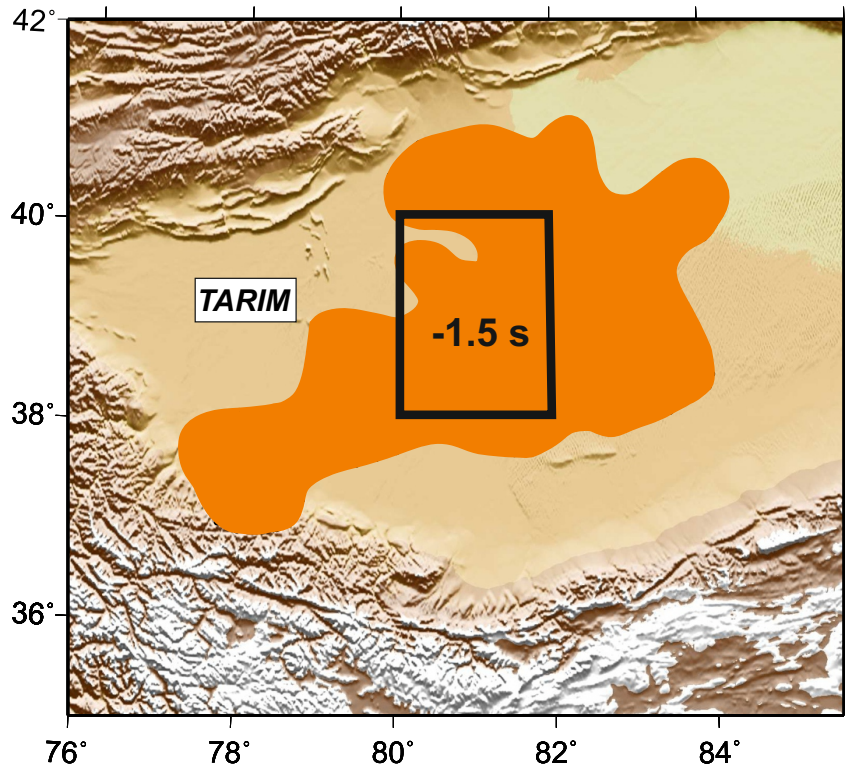




Figure 5

